

On Qualitative Analysis of Lattice Dynamical System of Two- and Three-Dimensional Biopixels Array: Bifurcations and Transition to “Chaos”



Oleksandr Nakonechnyi, Vasyl Martsenyuk, Mikolaj Karpinski,
and Aleksandra Klos-Witkowska

Abstract We consider the model of two- or three-dimensional biopixels array, which can be used for design of biosensors. The model is based on the system of lattice differential equations with time delay, describing interactions of biological species of neighbouring pixels. The qualitative analysis includes permanence and extinctions of solutions, stability investigation, bifurcations and transition to chaos. The stability conditions are obtained with help of the method of Lyapunov functionals. They are formulated in terms of the value of time necessary for immune response. Numerical research is presented with the help of phase portraits, square and hexagonal lattice plots and bifurcation diagrams.

Keywords Biopixels array · Delayed dynamic system · Qualitative analysis

1 Introduction

Nowadays, reaction-diffusion models are used in designing and studies of a lot of detecting, measuring and sensing devices. Immunosensor, which are studied here as an example, is kind of them. Such spatial-temporal models are described by the systems of partial or lattice differential equations.

O. Nakonechnyi

Department of Systems Analysis and Decision Making Theory, Taras Shevchenko National University of Kyiv, Kyiv, Ukraine

<https://csc.knu.ua/uk/person/nakonechniy>

V. Martsenyuk (✉) · M. Karpinski · A. Klos-Witkowska

Department of Computer Science and Automatics, University of Bielsko-Biala, Bielsko-Biala, Poland

e-mail: vmartsenyuk@ath.bielsko.pl; <http://www.kinf.ath.bielsko.pl/pl/vasyl-martsenyuk>;
mkarpinski@ath.bielsko.pl; <http://www.kinf.ath.bielsko.pl/pl/mikolaj-karpinski>;
awitkowska@ath.bielsko.pl; <http://www.kinf.ath.bielsko.pl/pl/aleksandra-klos-witkowska>

© Springer Nature Switzerland AG 2021

J. Awrejcewicz (ed.), *Perspectives in Dynamical Systems III: Control and Stability*,

Springer Proceedings in Mathematics & Statistics 364,

https://doi.org/10.1007/978-3-030-77314-4_3

The biosensor models are traditionally studied from the viewpoint of their qualitative analysis. Even in case of a small number of spatial elements they show complex behavior. In [1] it was shown that the model describing the chemical reaction of two morphogens (reactants), one of them diffusing within two compartments, results in “bi-chaotic” behavior. The origin of such chaotic phenomena¹ were also explained with help of statistics of topological defects [2].

When considering continuously distributed reaction-diffusion models described by nonlinear partial differential equations, Feigenbaum-Sharkovskii-Magnitskii bifurcation theory can be applied, which results in a subharmonic cascade of bifurcations of stable limit cycles [3].

The lattice differential equations describes the systems with the discrete spatial structure, which is more consistent with pixel devices. These equations were also called earlier by a series of authors as spatially discrete differential equations [4].

In [5] a lattice differential equation was presented in the form

$$\dot{u}_\xi = g_\xi(\{u_\zeta\}_{\zeta \in \Lambda}), \xi \in \Lambda, \quad (1)$$

where a lattice $\Lambda \subset \mathbb{R}^n$ can be determined as a discrete subset of \mathbb{R}^n , arranged in accordance with some regular spatial structure. Here u_ξ , $\xi \in \Lambda$ are the values of $u = \{u_\xi\}_{\xi \in \Lambda}$ at the points of the lattice, g_ξ are the right sides of the equations enabling us the existence of solution.

As a rule, without loss of generality, they consider $\Lambda = \mathbb{Z}^n$, which is the integer lattice in \mathbb{R}^n . The methods developed can be easily applied to a different type of lattices, namely, the planar rectangular and hexagonal lattice, the crystallographic lattices in \mathbb{R}^3 .

They pay an attention to the notion of delay in lattice differential equations, so-called delayed lattice differential equations. One of the application dealing with them is the investigation of traveling wave fronts and their stability [5]. The main results are applied to the delayed and discretely diffusive models for the population (see, e.g. [6, 7]).

Lattice differential equations are used as models in a lot of applications, for example, cellular neural networks, image processing, chemical kinetics, material science, in particular metallurgy, and biology [5, 8]. Lattice models are extremely attractive from viewpoint of population dynamics especially in case of spatially separated populations [5, 6, 8–11].

There are few reasons requiring consideration the hexagonal grid instead of rectangular ones (primarily in image and vision computing). Namely, the equal distances between neighboring pixels for hexagonal coordinate systems [12]; hexagonal points are packed more densely [13]; since the “hexagons are ‘rounder’ than squares”, the presentation of curves are more consistent with help of hexagonal systems [13]; hence, mathematical operations of edge detection and shape extraction are more successfully when applying hexagonal lattices [14].

¹They call it as “spiral turbulence” [2].

With the purpose of indexing hexagonal pixels, as a rule, they use two² or three-element³ coordinate systems [15]. Our reasonings will be based on the last one. In contrary to skewed axes, the using of the cubic coordinates enables us symmetries with respect to all three axes.

2 Lattice Model of Antibody-Antigen Interaction for Two-Dimensional Biopixels Array

Let $V_{i,j}(t)$ be concentration of antigens, $F_{i,j}(t)$ be concentration of antibodies in biopixel (i, j) , $i, j = \overline{1, N}$ (Fig. 1).

The model is based on the following biological assumptions for arbitrary biopixel (i, j) .

1. We have some constant birthrate $\beta > 0$ for antigen population.
2. Antigens are detected, binded and finally neutralized by antibodies with some probability rate $\gamma > 0$.

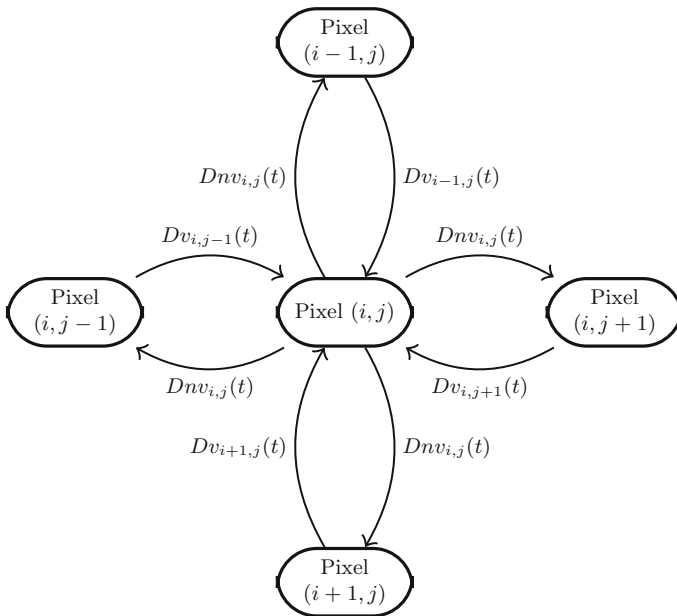


Fig. 1 Linear lattice interconnected four neighboring pixels model, $n > 0$ is disbalance constant

²So called “skewed-axis” coordinate system.

³It is also known as “cube hex coordinate system”.

3. We have some constant death rate of antibodies $\mu_f > 0$.
4. We assume that when the antibody colonies are absent, the antigen colonies are governed by the well known delay logistic equation:

$$\frac{dV_{i,j}(t)}{dt} = (\beta - \delta_v V_{i,j}(t - \tau))V_{i,j}(t), \quad (2)$$

where β and δ_v are positive numbers and $\tau \geq 0$ denotes delay in the negative feedback of the antigen colonies.

5. The antibody decreases the average growth rate of antigen linearly with a certain time delay τ ; this assumption corresponds to the fact that antibodies cannot detect and bind antigen instantly; antibodies have to spend τ units of time before they are capable of decreasing the average growth rate of the antigen colonies; these aspects are incorporated in the antigen dynamics by the inclusion of the term $-\gamma F_{i,j}(t - \tau)$ where γ is a positive constant which can vary depending on the specific colonies of antibodies and antigens.
6. In case of the lack of antigen colonies, the average growth rate of the antibody colonies decreases exponentially due to the presence of $-\mu_f$ in the antibody dynamics, and to incorporate the negative effects of antibody crowding, we have included the term $-\delta_f F_{i,j}(t)$ in the antibody dynamics.
7. The positive feedback $\eta\gamma V_{i,j}(t - \tau)$ in the average growth rate of the antibody has a delay since mature adult antibodies can only contribute to the production of antibody biomass; one can consider the delay τ in $\eta\gamma V_{i,j}(t - \tau)$ as a delay in antibody maturation.
8. While the last delay need not be the same as the delay in the hunting term and in the term governing antigen colonies, we have retained this for simplicity. We remark that the delays in the antibody term, antibody replacement term and antigen negative feedback term can be made different and a similar analysis can be followed.
9. We have some diffusion of antigens from four neighboring pixels $(i - 1, j)$, $(i + 1, j)$, $(i, j - 1)$, $(i, j + 1)$ (see Fig. 4) with diffusion $D > 0$. Here we consider only diffusion of antigens, because the model describes so-called “competitive” configuration of immunosensor [16]. When considering competitive configuration of immunosensor, the factors immobilized on the biosensor matrix are antigens, while the antibodies play the role of analytes or particles to be detected.
10. We consider surface lateral diffusion (movement of molecules on the surface on solid phase toward an immobilized molecules) [17]. Moreover, there are works [18, 19] which assume and consider surface diffusion as an entirely independent stage.
11. We extend definition of usual diffusion operator in case of surface diffusion in the following way. Let $n \in (0, 1]$ be a factor of diffusion disbalance. It means that only n th portion of antigens of the pixel (i, j) may be included into diffusion process to any neighboring pixel as a result of surface diffusion.

For the reasonings given we consider a very simple delayed antibody-antigen competition model for biopixels two-dimensional array which is based on well-known Marchuk model [20–23] and using spatial operator \hat{S} offered in [24] (Supplementary information, p.10)

$$\begin{aligned} \frac{dV_{i,j}(t)}{dt} &= (\beta - \gamma F_{i,j}(t - \tau) - \delta_v V_{i,j}(t - \tau))V_{i,j}(t) + \hat{S}\{V_{i,j}\}, \\ \frac{dF_{i,j}(t)}{dt} &= (-\mu_f + \eta\gamma V_{i,j}(t - \tau) - \delta_f F_{i,j}(t))F_{i,j}(t) \end{aligned} \quad (3)$$

with given initial functions

$$\begin{aligned} V_{i,j}(t) &= V_{i,j}^0(t) \geq 0, \quad F_{i,j}(t) = F_{i,j}^0(t) \geq 0, \quad t \in [-\tau, 0), \\ V_{i,j}(0), F_{i,j}(0) &> 0. \end{aligned} \quad (4)$$

For a square $N \times N$ array of traps, we use the following discrete diffusion form of the spatial operator [24]

$$\hat{S}\{V_{i,j}\} = \begin{cases} D[V_{1,2} + V_{2,1} - 2nV_{1,1}] & i, j = 1 \\ D[V_{2,j} + V_{1,j-1} + V_{1,j+1} - 3nV_{i,j}] & i = 1, j \in \overline{2, N-1} \\ D[V_{1,N-1} + V_{2,N} - 2nV_{1,N}] & i = 1, j = N \\ D[V_{i-1,N} + V_{i+1,N} + V_{i,N-1} - 3nV_{i,N}] & i \in \overline{2, N-1}, j = N \\ D[V_{N-1,N} + V_{N,N-1} - 2nV_{N,N}] & i = N, j = N \\ D[V_{N-1,j} + V_{N,j-1} + V_{N,j+1} - 3nV_{N,j}] & i = N, j \in \overline{2, N-1} \\ D[V_{N-1,1} + V_{N,2} - 2nV_{N,1}] & i = N, j = 1 \\ D[V_{i-1,1} + V_{i+1,1} + V_{i,2} - 3nV_{i,1}] & i \in \overline{2, N-1}, j = 1 \\ D[V_{i-1,j} + V_{i+1,j} + V_{i,j-1} + V_{i,j+1} - 4nV_{i,j}] & i, j \in \overline{2, N-1} \end{cases} \quad (5)$$

Each colony is affected by the antigen produced in four neighboring colonies, two in each dimension of the array, separated by the equal distance Δ . We use the boundary condition $V_{i,j} = 0$ for the edges of the array $i, j = 0, N + 1$. Further we will use the following notation of the constant

$$k(i, j) = \begin{cases} 2 & i, j = 1; \quad i = 1, j = N; \quad i = N, j = N; \quad i = N, j = 1, \\ 3 & i = 1, j \in \overline{2, N-1}; \quad i \in \overline{2, N-1}, j = N; \quad i = N, j \in \overline{2, N-1}; \\ & i \in \overline{2, N-1}, j = 1 \\ 4 & i, j \in \overline{2, N-1} \end{cases} \quad (6)$$

which will be used in manipulations with the spatial operator (5).

Results of modeling (3) are presented further. It can be seen that qualitative behavior of the system is determined mostly by the time of immune response τ (or time delay), diffusion D and constant n .

2.1 Stability Investigation

Steady States The steady states of the model (3) are the intersection of the nullclines $dV_{i,j}(t)/dt = 0$ and $dF_{i,j}(t)/dt = 0$, $i, j = \overline{1, N}$.

Antigen-Free Steady State If $V_{i,j}(t) \equiv 0$, the free antigen equilibrium is at $\mathcal{E}_{i,j}^0 \equiv (0, 0)$, $i, j = \overline{1, N}$ or $\mathcal{E}_{i,j}^0 \equiv (0, -\frac{\mu_f}{\delta_f})$, $i, j = \overline{1, N}$. The last solution does not have biological sense and can not be reached for nonnegative initial conditions (4).

When considering endemic steady state $\mathcal{E}_{i,j}^* \equiv (V_{i,j}^*, F_{i,j}^*)$, $i, j = \overline{1, N}$ for (3) we get algebraic system:

$$\begin{aligned} (\beta - \gamma F_{i,j}^* - \delta_v V_{i,j}^*) V_{i,j}^* + \hat{S} \{V_{i,j}^*\} &= 0, \\ (-\mu_f + \eta\gamma V_{i,j}^* - \delta_f F_{i,j}^*) F_{i,j}^* &= 0, \quad i, j = \overline{1, N}. \end{aligned} \quad (7)$$

The solutions $(V_{i,j}^*, F_{i,j}^*)$ of (7) can be found as a result of solving lattice equation with respect to $V_{i,j}^*$, and using relation $F_{i,j}^* = \frac{-\mu_f + \eta\gamma V_{i,j}^*}{\delta_f}$

Then we have to differ two cases.

Identical Endemic State for All Pixels Let's assume there is a solution of (7) $V_{i,j}^* \equiv V^*$, $F_{i,j}^* \equiv F^*$, $i, j = \overline{1, N}$, i.e., $\hat{S} \{V_{i,j}^*\} \equiv 0$. Then $\mathcal{E}_{i,j}^* = (V^*, F^*)$, $i, j = \overline{1, N}$ can be calculated as

$$V^* = \frac{-\beta\delta_f - \gamma\mu_f}{\delta_v\delta_f - \eta\gamma^2}, \quad F^* = \frac{\delta_v\mu_f - \eta\gamma\beta}{\delta_v\delta_f - \eta\gamma^2}. \quad (8)$$

provided that $\delta_v\delta_f - \eta\gamma^2 < 0$.

Nonidentical Endemic State for Pixels In general case we have endemic steady state which is different from (8). It is shown numerically in Appendix B that it appears as a result of diffusion between pixels D .

At absence of diffusion, i.e. $D = 0$, we have only identical endemic state for pixels of external layer. At presence of diffusion $D > 0$ nonidentical endemic states tends to identical one (8) at internal pixels, which can be observed at numerical simulation. This phenomenon is clearly appeared at bigger amount of pixels.

Basic Reproduction Numbers Here we define the basic reproduction number for antigen colony which is localized in pixel (i, j) . When considering epidemic models, the basic reproduction number, \mathcal{R}_0 , is defined as the expected number of secondary cases produced by a single (typical) infection in a completely susceptible population. It is important to note that \mathcal{R}_0 is a dimensionless number [25]. When applying this definition to the pixel (i, j) , which is described by the equation (3), we get

$$\mathcal{R}_{0,i,j} = \mathcal{T}_{i,j} \bar{c}_{i,j} d_{i,j}$$

where $\mathcal{T}_{i,j}$ is the transmissibility (i.e., probability of binding given constant between an antigen and antibody), $\bar{c}_{i,j}$ is the average rate of contact between antigens and antibodies, and $d_{i,j}$ is the duration of binding of antigen by antibody till deactivation.

Unfortunately, the lattice system (3) doesn't include all parameters, which allow to calculate the basic reproduction numbers in a clear form. Firstly, let's consider pixel (i^*, j^*) without diffusion, i.e., $\hat{S} \{V_{i^*,j^*}\} \equiv 0$. In this case the non-negative equilibria of (3) are

$$\mathcal{E}_{i^*,j^*}^0 = (V^0, 0) := \left(\frac{\beta}{\delta_v}, 0\right), \quad \mathcal{E}_{i^*,j^*}^* = (V^*, F^*).$$

Due to the approach which was offered in [26] (in pages 4 for ordinary differential equations, 5 for delay model), we introduce the basic reproduction number for pixel (i^*, j^*) without diffusion, which is given by expression

$$\mathcal{R}_{0,i^*,j^*} := \frac{V^0}{V^*} = \frac{\beta}{\delta_v V^*} = \frac{\beta(\eta\gamma^2 - \delta_v\delta_f)}{\delta_v(\beta\delta_f + \gamma\mu_f)}.$$

Its biological meaning is given as being the average number of offsprings produced by a mature antibody in its lifetime when introduced in a antigen-only environment with antigen at carrying capacity.

Following the approach of population dynamics it has to be shown that antibody-free equilibrium \mathcal{E}_{i^*,j^*}^0 is locally asymptotically stable if $\mathcal{R}_{0,i^*,j^*} < 1$ and it is unstable if $\mathcal{R}_{0,i^*,j^*} > 1$ (see, e.g. [27]). It can be done with help of analysis of the roots of characteristic equation (similarly to [26], p.5). Thus, $\mathcal{R}_{0,i^*,j^*} > 1$ is sufficient condition for existence of the endemic equilibrium \mathcal{E}_{i^*,j^*}^* .

We can consider the expression mentioned above for the general case of the lattice system (3), i.e., when considering diffusion. In this case we have the "lattice" of the basic reproduction numbers $\mathcal{R}_{0,i,j}$, $i, j = \overline{1, N}$ satisfying to

$$\mathcal{R}_{0,i,j} := \frac{V_{i,j}^0}{V_{i,j}^*}, \quad i, j = \overline{1, N}, \quad (9)$$

where $\mathcal{E}_{i,j}^0$, $i, j = \overline{1, N}$ are nonidentical steady states, which are found as a result of solution of the algebraic system

$$\left(\beta - \delta_v V_{i,j}^0\right) V_{i,j}^0 + \hat{S} \left\{ V_{i,j}^0 \right\} = 0, \quad i, j = \overline{1, N}, \quad (10)$$

endemic states $\mathcal{E}_{i,j}^* = \left(V_{i,j}^*, F_{i,j}^*\right)$, $i, j = \overline{1, N}$ are found using (7).

It is worth to say that due to the principles of population dynamics the conditions

$$\mathcal{R}_{0,i,j} > 1, \quad i, j = \overline{1, N} \quad (11)$$

have to be sufficient for the existence of endemic state $\mathcal{E}_{i,j}^*$. We will check it only with help of numerical simulations.

2.2 Persistence of the Solutions

We will use the following definition which generalizes [28] for lattice differential equations.

Definition 1 System (3) is said to be uniformly persistent if for all $i, j = \overline{1, N}$ there exist compact regions $\mathcal{D}_{i,j} \subset \text{int}\mathbb{R}^2$ such that every solution $(V_{i,j}(t), F_{i,j}(t))$, $i, j = \overline{1, N}$ of (3) with the initial conditions (4) eventually enters and remains in the region $\mathcal{D}_{i,j}$.

Theorem 1 Let $(V_{i,j}(t), F_{i,j}(t))$, $i, j = \overline{1, N}$ be the solutions of (3) with initials conditions (4). If

$$\beta\eta\gamma - \mu_f\delta_v > 0, \quad (12)$$

then

$$0 < V_{i,j}(t) \leq M_v, \quad 0 < F_{i,j}(t) \leq M_f \quad (13)$$

for some large values of t . Here

$$M_v = \frac{\beta}{\delta_v} e^{\beta\tau}, \quad M_f = \frac{1}{\delta_f} \left(\eta\gamma M_v - \mu_f \right). \quad (14)$$

Proof Firstly, we can prove that there exists some large instant of time T_1 that $\hat{S}\{V_{i,j}(t)\} \leq 0$, $i, j = \overline{1, N}$, $t > T_1$.

Let's assume the contrary, i.e. there is $i^*, j^* \in \overline{1, N}$, that $\hat{S}\{V_{i,j}(t)\} > 0$ at $t > T_1$, which is a contradiction with a balance principle.

Since the solutions of the system (3), (4) are positive, then

$$\frac{dV_{i,j}(t)}{dt} \leq \left(\beta - \delta_v V_{i,j}(t - \tau) \right) V_{i,j}(t). \quad (15)$$

Further we can apply the basic steps of proof of Lemma 3.1 [29] which is proved in nonlattice case (i.e. without spatial operator).

Remark 1 Conditions of uniform persistence of system (3) in nonlattice case were obtained in [30]. They resulted in inequality (12) provided that

$$\beta \delta_f + \mu_f \gamma > 0 \quad (16)$$

holds.

2.3 Extinction Research

The next result introduces a sufficient condition for the underlying grid size ensuring that the solution of (3) is non-vanishing.

Theorem 2 *Let for the system (3) the positive orthant Ω be positive invariant. Besides that, let N be such that $f_{\text{extnc}}(N) < 1$ holds, where*

$$f_{\text{extnc}}(N) = \max_{k,l=1,N} \left| \beta - \frac{4D}{\Delta^2} \left(1 + \cos \frac{\pi(k+l)}{2(N+1)} \cos \frac{\pi(k-l)}{2(N+1)} \right) \right|. \quad (17)$$

Then $\lim_{t \rightarrow \infty} V_{i,j}(t) = 0$, $i, j = \overline{1, N}$.

Proof It requires a comparison principle for differential equations.

The following inequalities hold for $V_{i,j}(t)$

$$\frac{V_{i,j}(t)}{dt} < \beta V_{i,j}(t) + \hat{S} \{V_{i,j}(t)\}.$$

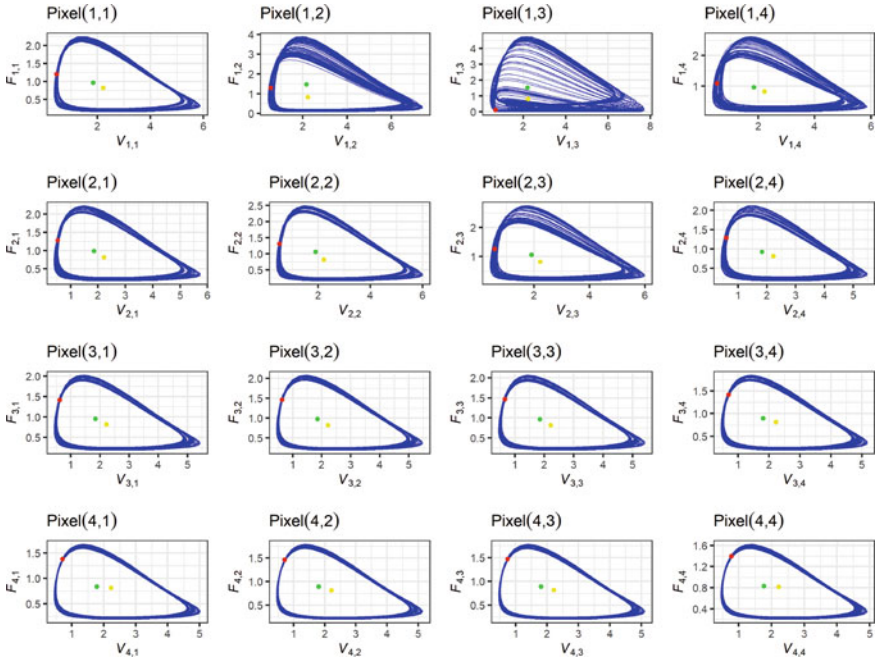
Consider N^2 -vector of the form

$$V(n) = \left(V_{1,1}(t), V_{1,2}(t), \dots, V_{1,N}(t), V_{2,1}(t), \dots, V_{2,N}(t), \dots, \right. \\ \left. V_{N,1}(t), \dots, V_{N,N}(t) \right)^{\top}.$$

Table 1 The values of $R_{0,i,j}$, $i, j = 1, 4$

$R_{0,i,j}^*$	1	2	3	4
1	3.218727	3.425273	3.474323	3.224824
2	3.171270	3.235043	3.236289	3.126438
3	3.092287	3.107824	3.096617	3.040443
4	2.997269	3.020902	3.012915	2.971442

Table 2 The phase plane plots of the system (3) for antibody populations $F_{i,j}$ versus antigen populations $V_{i,j}$, $i, j = 1, 4$. Numerical simulation of the system (3) at $n = 0.9$, $\tau = 0.28725$. Here ● indicates identical steady state, ● indicates nonidentical steady state. Trajectories are constructed for $t \in [550, 800]$. The solution behavior looks chaotic



The numerical simulations were implemented at different values of $n \in (0, 1]$. Here we can see that when changing the value of τ we have changes of qualitative behavior of pixels and entire immunosensor. We considered the parameter value set given above and computed the long-time behavior of the system (3) for $\tau = 0.05, 0.22, 0.23, 0.2865$, and 0.28725 . The phase diagrams of the antibody vs. antigen populations for the pixel (1, 1) are shown in Table 2.

For example, at $\tau \in [0, 0.22]$ we can see trajectories corresponding to stable node for all pixels.

For $\tau = 0.23$, the phase diagrams show that the solution is a limit cycle with two local extrema (one local maximum and one local minimum) per cycle. Then for $\tau = 0.2825$ the solution is a limit cycle with four local extrema per cycle, and, for $\tau = 0.2868, 0.2869, 0.28695$ the solutions are limit cycles with 8, 16 and 32

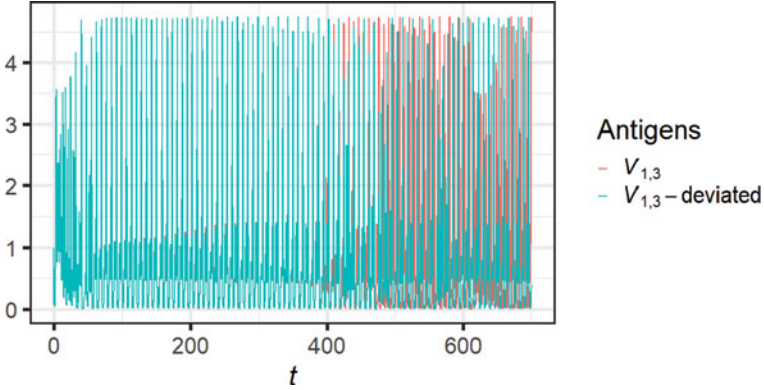


Fig. 2 The time series of the solutions to the system (3) for the antigen population $V_{1,3}$ from $t = 0$ to 700 with $\tau = 0.28725$ for initial conditions $V_{1,3}(t) = 1$ and $V_{1,3}(t) = 1.001$ (deviated), $t \in [-\tau, 0]$, and identical all the rest ones. At the beginning the two solutions appear to be the same, but as time increases there is a marked difference between the solutions supporting the conclusion that the system behavior is chaotic

local extrema per cycle, respectively. Finally, for $\tau = 0.28725$, the behavior shown in Table 2 is obtained which looks like chaotic behavior. In this paper, we have regarded behavior as chaotic if no periodic behavior could be found in the long-time behavior of the solutions.

The divergence of nearby trajectories in phase space is one of the most striking properties of chaotic behavior of deterministic systems [32]. In order to evaluate that the solution is chaotic for $\tau = 0.28725$, we perturbed the initial conditions to test the sensitivity of the system. Figure 2 presents two trajectories (in red and blue) starting from initial conditions with a small deviation (0.001). It can be seen that till the moment about $t = 400$ there is no significant difference between the trajectories, whereas further nearby trajectories are being deviated. The divergence of the trajectories with the small initial deviation evidences numerically the chaotic behavior at $\tau = 0.28725$.

We have also checked numerically that the solutions for the limit cycles are periodic and computed the periods for each of the local maxima and minima in the cycles. In the chaotic solution region, the numerical calculations (not shown in this paper) confirmed that no periodic behavior could be found.

A bifurcation diagram showing the maximum and minimum points for the limit cycles for the antigen population $V_{1,3}$ as a function of time delay is given in Fig. 3. The Hopf bifurcation from the stable equilibrium point to a simple limit cycle and the sharp transitions at critical values of the time delay between limit cycles with increasing numbers of maximum and minimum points per cycle can be clearly seen.

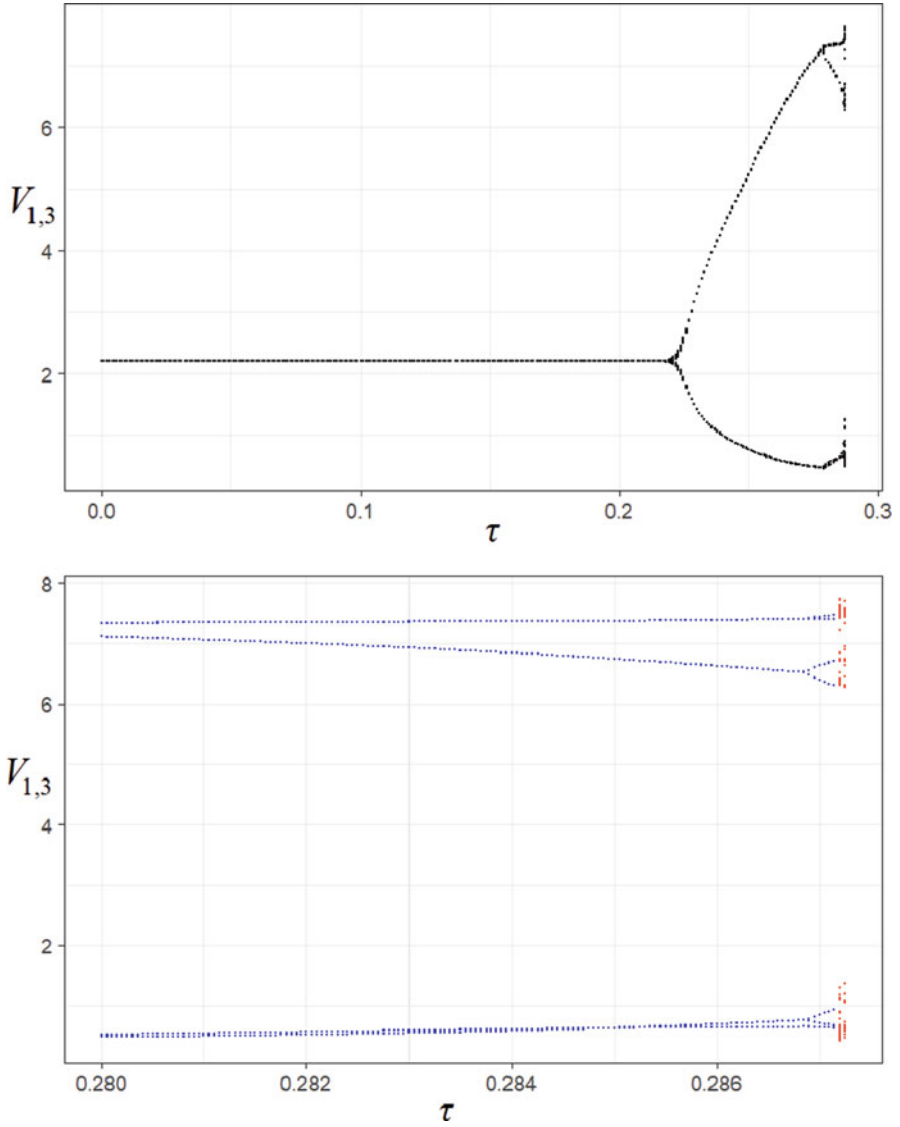


Fig. 3 A bifurcation diagram showing the “bifurcation path to chaos” as the time delay is increased. The points show the local extreme points per cycle for the $V_{1,3}$ population. Chaotic-type solutions occur at $\tau \approx 0.28725$ and are indicated in red in the figure with value 0 for the number of extreme points

3 Three-Dimensional Biopixels Array

When modeling three-dimensional pixels array it is natural way to apply the model based on the hexagonal lattice. Such model may use the following assumption. Namely, antigens are assumed to diffuse from six neighboring pixels, $(i + 1, j, k - 1)$, $(i + 1, j - 1, k)$, $(i, j - 1, k + 1)$, $(i - 1, j, k + 1)$, $(i - 1, j + 1, k)$, $(i, j + 1, k - 1)$ (see Fig. 4), with diffusion rate $D\Delta^{-2}$, where $D > 0$ and $\Delta > 0$ is distance between pixels.

Taking into account prerequisites mentioned above, we get a simplified antibody-antigen competition model with delay for a hexagonal array of biopixels, which uses Marchuk model of the immune response [20–23] and using spatial operator \hat{S} which is constructed similarly to [24] (Supplementary information, p.10)

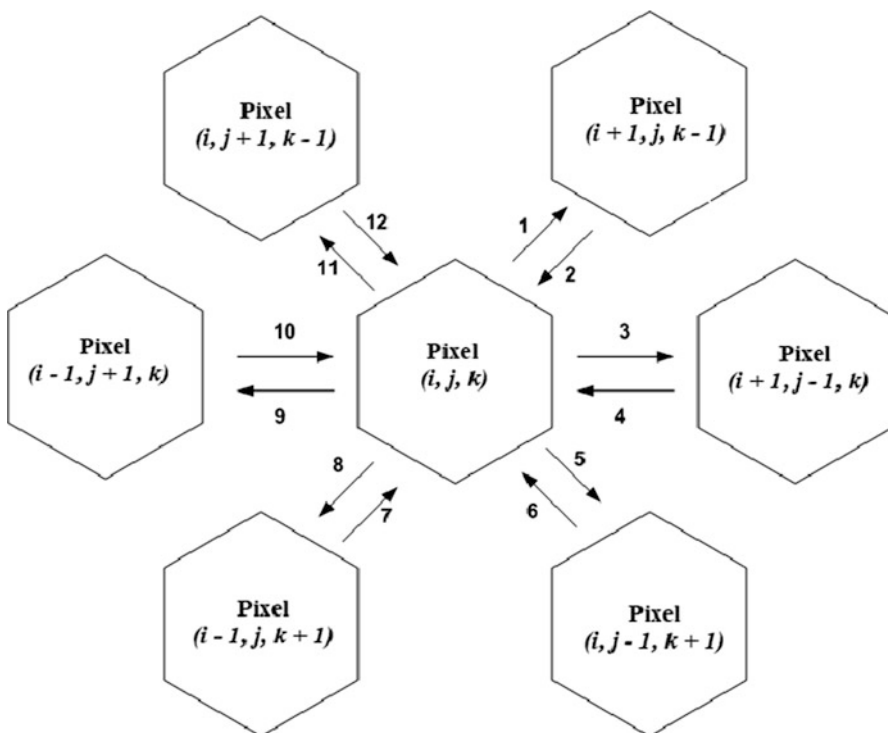


Fig. 4 Diffusion of antigens for the hexagonal lattice model. Antigens from six neighboring pixels interact, $n > 0$ is the constant of disbalance. Here ‘1’, ‘3’, ‘5’, ‘8’, ‘9’, ‘11’ have to be replaced with $D\Delta^{-2}V_{i,j,k}(t)$, ‘2’ with $D\Delta^{-2}V_{i+1,j,k-1}(t)$, ‘4’ with $D\Delta^{-2}V_{i+1,j-1,k}(t)$, ‘6’ with $D\Delta^{-2}V_{i,j-1,k+1}(t)$, ‘7’ with $D\Delta^{-2}V_{i-1,j,k+1}(t)$, ‘10’ with $D\Delta^{-2}V_{i-1,j+1,k}(t)$, ‘12’ with $D\Delta^{-2}V_{i,j+1,k-1}(t)$

$$\begin{aligned} \frac{dV_{i,j,k}(t)}{dt} &= (\beta - \gamma F_{i,j,k}(t - \tau) - \delta_v V_{i,j,k}(t - \tau)) V_{i,j,k}(t) + \hat{S}\{V_{i,j,k}\}, \\ \frac{dF_{i,j,k}(t)}{dt} &= (-\mu_f + \eta\gamma V_{i,j,k}(t - \tau) - \delta_f F_{i,j,k}(t)) F_{i,j,k}(t) \end{aligned} \quad (18)$$

with given initial functions

$$\begin{aligned} V_{i,j,k}(t) &= V_{i,j,k}^0(t) \geq 0, \quad F_{i,j,k}(t) = F_{i,j,k}^0(t) \geq 0, \quad t \in [-\tau, 0), \\ V_{i,j,k}(0), F_{i,j,k}(0) &> 0. \end{aligned} \quad (19)$$

We use the following spatial operator of discrete diffusion for a hexagonal array of pixels⁴

$$\begin{aligned} \hat{S}\{V_{i,j,k}\} &= D\Delta^{-2} \left[V_{i+1,j,k-1} + V_{i+1,j-1,k} + V_{i,j-1,k+1} + V_{i-1,j,k+1} + V_{i-1,j+1,k} \right. \\ &\quad \left. + V_{i,j+1,k-1} - 6nV_{i,j,k} \right] \\ i, j, k &\in \overline{-N+1, N-1}, \quad i+j+k=0. \end{aligned} \quad (20)$$

Each pixel is affected by the antigens flowing out six neighboring pixels, two in each of three directions of the hexagonal array. The adjoint pixels are separated by the distance Δ .

Boundary conditions $V_{i,j,k} = 0$ for the edges of the hexagonal array, i.e. if $i \vee j \vee k \in \{-N-1, N+1\}$, are used.

We can present analytical results with respect to the model (18) in the form of restrictions for the parameters, enabling us persistence and global asymptotic stability. Moreover, we executed numerical research of the system qualitative behavior in dependence of changes of the time of immune response τ (delay of time), diffusion rate $D\Delta^{-2}$ and factor n .

3.1 Persistence and Extinction of the Solutions

Concerning persistence, for the hexagonal lattice can be obtained similar result as for square one (Theorem 1), just adding the third index.

Unfortunately, we didn't manage to present such clear condition of extinction as in Theorem 2. We can check it only numerically in an experimental way.

⁴Without loss of generality we consider spatial operator for internal pixels only.

3.2 Numerical Study

For numerical simulation we consider model (18) of hexagonal pixels array at $N = 4$, $\beta = 2 \text{ min}^{-1}$, $\gamma = 2 \frac{\text{mL}}{\text{min} \cdot \mu\text{g}}$, $\mu_f = 1 \text{ min}^{-1}$, $\eta = 0.8/\gamma$, $\delta_v = 0.5 \frac{\text{mL}}{\text{min} \cdot \mu\text{g}}$, $\delta_f = 0.5 \frac{\text{mL}}{\text{min} \cdot \mu\text{g}}$, $D = 0.2 \frac{\text{nm}^2}{\text{min}}$, $\Delta = 0.3 \text{ nm}$. Numerical modeling was implemented at different values of $n \in (0, 1]$. For this purpose we used RStudio environment.

Using local bifurcation plot, dynamics of the system (18) was analysed for different values of $n \in (0, 1]$. We have concluded that oscillatory and then chaotic behavior starts for smaller values of τ at smaller values of n . Further, increasing the values of n we can observe asymptotically stable steady solutions for wider range of τ .

Numerical integration of the system has shown the influence of time delay τ . Namely, as it is agreed with the analytical results, we observe the stable focuses at pixel-dependent endemic states for small delays $\tau \in [0, 0.18)$. At $\tau \approx 0.18 \text{ min}$ the stable focus is transformed into a stable limit cycle of tiny radius, which corresponds to Hopf bifurcation. A deeper study of this phenomenon requires obtaining the condition of the appearance of the pair of purely imaginary roots of the characteristic quasipolynomial of the linearized system. The limit cycles of ellipsoidal form are observed till $\tau \approx 0.285 \text{ min}$. Pay attention that when increasing τ , near $\tau = 0.285$ we get period doubling (see Fig. 5).⁵

Qualitative behavior of immunosensor model can be analyzed with help of hexagonal tiling plots also. For this purpose we can use both plots for antigens (Fig. 6), antibodies (Fig. 7) and probabilities of binding antigens by antibodies (Fig. 8).

4 Conclusions

In the work a reaction-diffusion models of two- and three-dimensional immunopixels array were considered. Mathematically it is described by the system of lattice delayed differential equations on rectangular or hexagonal grids. The systems include the spatial operator describing diffusion of antigenes between five and seven neighboring pixels respectively.

The main results are dealing with qualitative investigation of the model. The conditions of persistence were obtained. Also we have managed to get the result dealing with the extinction of the solutions. Namely, it can be seen that the amount of pixels determines their non-vanishing. In two-dimensional case this dependence can be presented in a clear form.

The conditions of local or global asymptotic stability can be obtained using construction of the Lyapunov functional. Because of cumbersome of evidence, we

⁵It can be approximately seen from local bifurcation plot also.

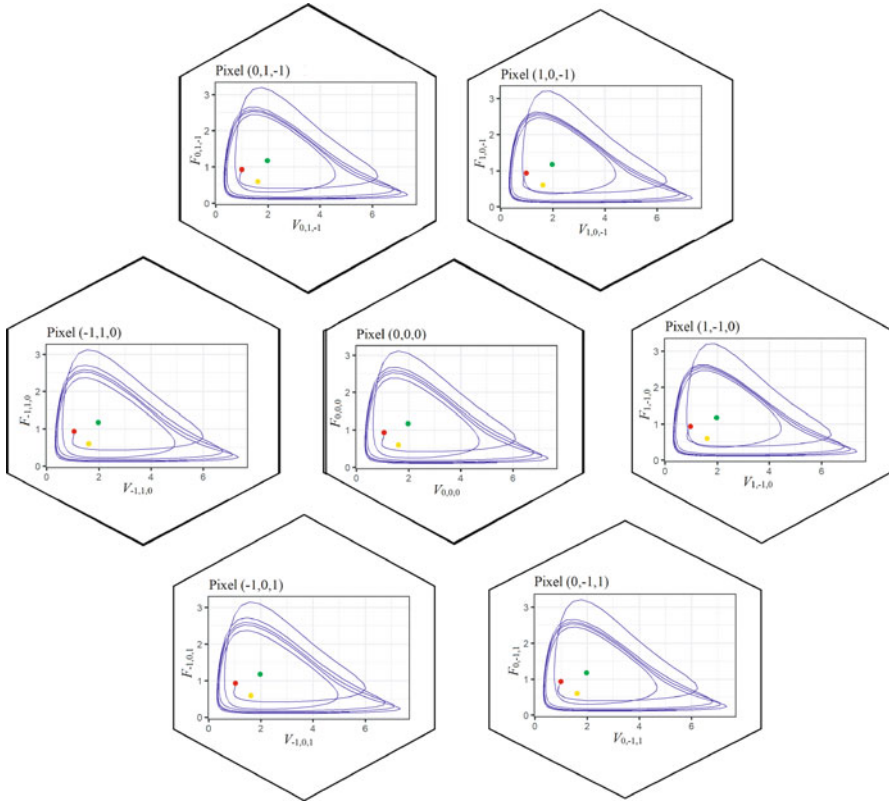


Fig. 5 Phase plots of the system (18) at $\tau = 0.287$. Here \bullet indicates initial state, \circ indicates pixel-independent endemic state, \circ indicates pixel-dependent endemic state. The solution tends to a stable limit cycle with six local extrema per cycle

didn't include it here. They results in inequality including the system parameters and delay. So, estimation of the delay enabling us local or global asymptotic stability can be obtained.

Numerical analysis of the model qualitative behavior is performed with the help of the bifurcation diagram, phase trajectories, and rectangular or hexagonal tile portraits. It has shown the changes in qualitative behavior with respect to the growth of time delay. Namely, starting from the stable focus at small delay values, then through Hopf bifurcation to limit cycles, and finally through period doublings to deterministic chaos. It is agreed with the results on spatial-temporal chaos for reaction-diffusion systems, which were previously obtained in [1–3].

As compared with rectangular lattice model, for hexagonal model we observe Hopf bifurcation at smaller values of τ . That is hexagonal lattice accelerates changes in qualitative behavior.

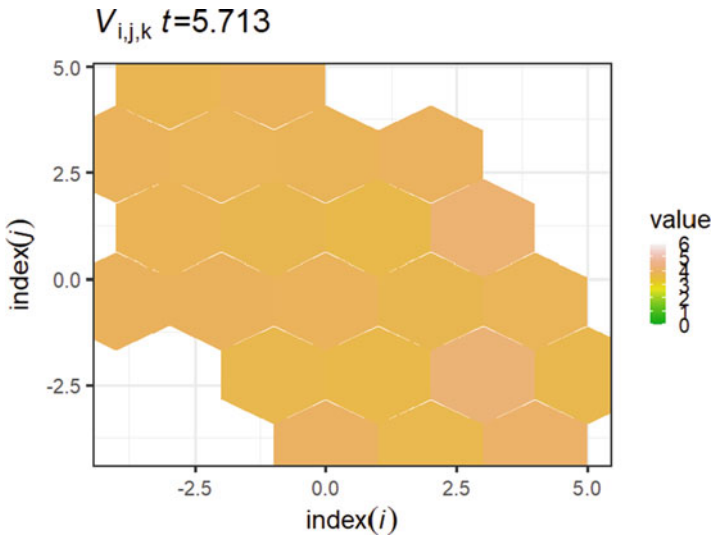


Fig. 6 Example of hexagonal tiling plot for V

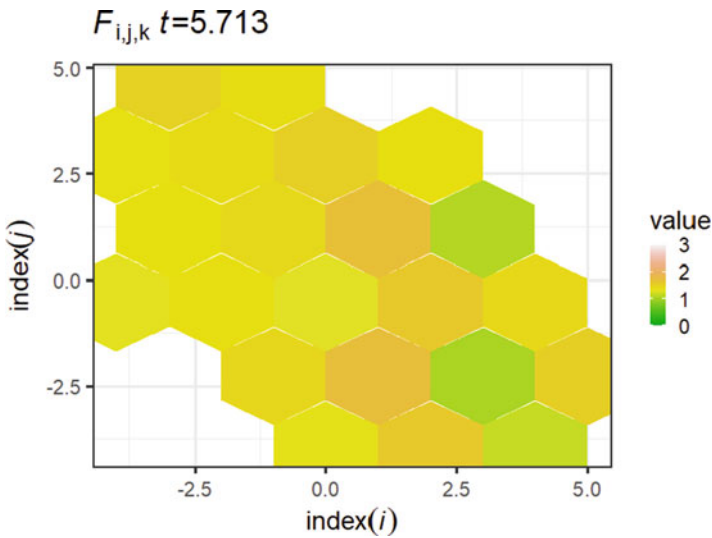


Fig. 7 Example of hexagonal tiling plot for F

Note, that model can be applied for an arbitrary amount of pixels determined by natural $N \geq 1$. However, it can be numerically seen that qualitative behavior of the entire immunosensor is determined by 5 or 7 pixels array for square and hexagonal lattices respectively.

The results of the work differ from the results presented earlier since here we try to show a comparative study of the model of biopixels array both in square

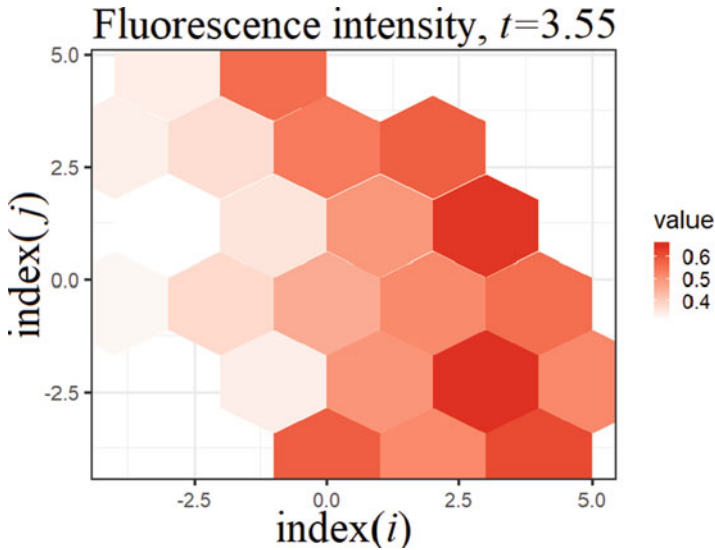


Fig. 8 Example of hexagonal tiling plot for probabilities of binding antigens by antibodies, i.e. $V \times F$. In case of optical immunosensor it is fluorescence intensity

and hexagonal lattices. Such a comparative study is based on both analytical and numerical results. Analytical outcomes include a comparison of the basic stability characteristics like basic reproductive numbers, a comparison of the conditions for persistence (permanence), and extinction. Numerical analysis use phase portraits and bifurcation plots which are constructed on the basis of local extremes. Earlier such studies were executed focusing on some type of the lattice. So, here we investigate the effect of the lattice type on the qualitative behavior of the model.

References

1. Rössler, O.E.: Chemical turbulence: Chaos in a simple reaction-diffusion system. *Zeitschrift für Naturforschung A* **31**(10), (1976). <https://doi.org/10.1515/zna-1976-1006>
2. Hildebrand, M., Bär, M., Eiswirth, M.: Statistics of topological defects and spatiotemporal chaos in a reaction-diffusion system. *Phys. Rev. Lett.* **75**(8), 1503–1506 (1995). <https://doi.org/10.1103/physrevlett.75.1503>
3. Zaitseva, M.F., Magnitskii, N.A.: Space-time chaos in a system of reaction-diffusion equations. *Differential Equations* **53**(11), 1519–1523 (2017). <https://doi.org/10.1134/s0012266117110155>
4. Cahn, J.W., Chow, S.N., Van Vleck, E.S.: Spatially discrete nonlinear diffusion equations. *Rocky Mount. J. Math.* **25**(1), 87–118 (1995)
5. Chow, S.-N., Mallet-Paret, J., Van Vleck, E.S.: Dynamics of lattice differential equations. *Int. J. Bifur. Chaos* **6**(09), 1605–1621 (1996)
6. Pan, S.: Propagation of delayed lattice differential equations without local quasimonotonicity. Preprint (2014). ArXiv:1405.1126.

7. Huang, J., Lu, G., Zou, X.: Existence of traveling wave fronts of delayed lattice differential equations. *J. Math. Anal. Appl.* **298**(2), 538–558 (2004)
8. Niu, H.: Spreading speeds in a lattice differential equation with distributed delay. *Turkish J. Math.* **39**(2), 235–250 (2015)
9. Hoffman, A., Hupkes, H., Van Vleck, E.: Entire Solutions for Bistable Lattice Differential Equations with Obstacles. American Mathematical Society, Rhode Island (2017)
10. Wu, F.: Asymptotic speed of spreading in a delay lattice differential equation without quasimonotonicity. *Electron. J. Differ. Equ.* **2014**(213), 1–10 (2014)
11. Zhang, G.-B.: Global stability of traveling wave fronts for non-local delayed lattice differential equations. *Nonlinear Anal. Real World Appl.* **13**(4), 1790–1801 (2012)
12. Luczak, Ed., Rosenfeld, A.: Distance on a hexagonal grid. *IEEE Trans. Comput.* **25**(5), 532–533 (1976). <https://doi.org/10.1109/TC.1976.1674642>
13. Hexagonal Coordinate Systems.: https://homepages.inf.ed.ac.uk/rbf/CVonline/LOCAL_COPIES/AV0405/MARTIN/Hex.pdf. Accessed: 2019-05-12
14. Middleton, L., Sivaswamy, J.: Edge detection in a hexagonal-image processing framework. *Image Vis. Comput.* **19**(14), 1071–1081 (2001)
15. Fayas, A., Nisar, H., Sultan, A.: Study on hexagonal grid in image processing. In: *The 4th International Conference on Digital Image Processing*, pp. 7–8 (2012)
16. Cruz, H.J., Rosa, C.C., Oliva, A.G.: Immunosensors for diagnostic applications. *Parasitology Research* **88**, S4–S7 (2002)
17. Paek, S.-H., Schramm, W.: Modeling of immunosensors under nonequilibrium conditions: I. mathematic modeling of performance characteristics. *Analytical Biochemistry* **196**(2), 319–325 (1991)
18. Bloomfield, V.A., Prager, S.: Diffusion-controlled reactions on spherical surfaces. application to bacteriophage tail fiber attachment. *Biophysical Journal* **27**(3), 447–453 (1979)
19. Berg, O.G.: Orientation constraints in diffusion-limited macromolecular association. the role of surface diffusion as a rate-enhancing mechanism. *Biophysical Journal* **47**(1), 1–14 (1985)
20. Marchuk, G.I., Petrov, R.V., Romanyukha, A.A., Bocharov, G.A.: Mathematical model of antiviral immune response. i. data analysis, generalized picture construction and parameters evaluation for hepatitis b. *J. Theor. Biol.* **151**(1), 1–40 (1991). [https://doi.org/10.1016/S0022-5193\(05\)80142-0](https://doi.org/10.1016/S0022-5193(05)80142-0). <https://www.scopus.com/inward/record.uri?eid=2-s2.0-0025819779&doi=10.1016%2fS0022-5193%2805%2980142-0&partnerID=40&md5=f850637085913dc18f8e52c5b3f28600> Cited By 38
21. Foryś, U.: Marchuk’s model of immune system dynamics with application to tumour growth. *J. Theor. Med.* **4**(1), 85–93 (2002). <https://doi.org/10.1080/10273660290052151>. <https://www.tandfonline.com/doi/abs/10.1080/10273660290052151>
22. Nakonechny, A.G., Marzeniuk, V.P.: Uncertainties in medical processes control. *Lect. Notes Econ. Math. Syst.* **581**, 185–192 (2006). https://doi.org/10.1007/3-540-35262-7_11. https://www.scopus.com/inward/record.uri?eid=2-s2.0-53749093113&doi=10.1007%2f3-540-35262-7_11&partnerID=40&md5=03be7ef103cbbc1e94cacbb471daa03f Cited By 2
23. Marzeniuk, V.P.: Taking into account delay in the problem of immune protection of organism. *Nonlinear Anal. Real World Appl.* **2**(4), 483–496 (2001). [https://doi.org/10.1016/S1468-1218\(01\)00005-0](https://doi.org/10.1016/S1468-1218(01)00005-0). <https://www.scopus.com/inward/record.uri?eid=2-s2.0-0041331752&doi=10.1016%2fS1468-1218%2801%2900005-0&partnerID=40&md5=9943d225f352151e77407b48b18ab1a9>. Cited By 2
24. Prindle, A., Samayoa, P., Razinkov, I., Danino, T., Tsimring, L.S., Hasty, J.: A sensing array of radically coupled genetic ‘biopixels’. *Nature* **481**(7379), 39–44 (2011). <https://doi.org/10.1038/nature10722>
25. Jones, J.H.: Notes on R_0 . California: Department of Anthropological Sciences (2007)
26. Yang, J., Wang, X., Zhang, F.: A differential equation model of hiv infection of cd t-cells with delay. *Discrete Dynamics in Nature and Society* (2008)
27. Elaiw, A.M., Almatrafi, A.A., Hobiny, A.D.: Effect of antibodies on pathogen dynamics with delays and two routes of infection. *AIP Advances* **8**(6), 065104 (2018). <https://doi.org/10.1063/1.5029483>.

28. Kuang, Y.: Delay Differential Equations with Applications in Population Dynamics. Academic Press, New York (1993)
29. zhong He, X.: Stability and delays in a predator-prey system. *J. Math. Anal. Appl.* **198**(2), 355–370 (1996). <https://doi.org/10.1006/jmaa.1996.0087>
30. Wendi, W., Zhien, M.: Harmless delays for uniform persistence. *J. Math. Anal. Appl.* **158**(1), 256–268 (1991). [https://dx.doi.org/10.1016/0022-247X\(91\)90281-4](https://dx.doi.org/10.1016/0022-247X(91)90281-4)
31. Lancaster, P., Tismenetsky, M.: The Theory of Matrices: With Applications. Elsevier (1985)
32. Persson, P.B., Wagner, C.D.: General principles of chaotic dynamics. *Cardiovascular Research* **31**, 332–341 (1996). <https://cardiovascres.oxfordjournals.org/content/31/3/332.full-text.pdf>